Supporting Information: Interfacial polyelectrolyte complex spinning of cellulose nanofibrils for advanced bicomponent fibers

Matti S. Toivonen,[†] *Sauli Kurki-Suonio,*[†] *Wolfgang Wagermaier,*[§] *Ville Hynninen,*[†] *Sami Hietala,*[#] *and Olli Ikkala*[†]*

†Molecular Materials, Department of Applied Physics, Aalto University (previously Helsinki University of Technology), P.O. Box 15100, FIN-00076 Aalto, Espoo, Finland

[§]Department of Biomaterials, Max Planck Institute of Colloids and Interfaces, D-14424 Potsdam, Germany

[#]Department of Chemistry, University of Helsinki, P.O. Box 55, FIN-00014 HY, Helsinki, Finland

* Corresponding author: Olli.Ikkala@aalto.fi

KEYWORDS: Nanocellulose, cellulose nanofibrils, interfacial polyelectrolyte complexation, fiber spinning, bicomponent fiber

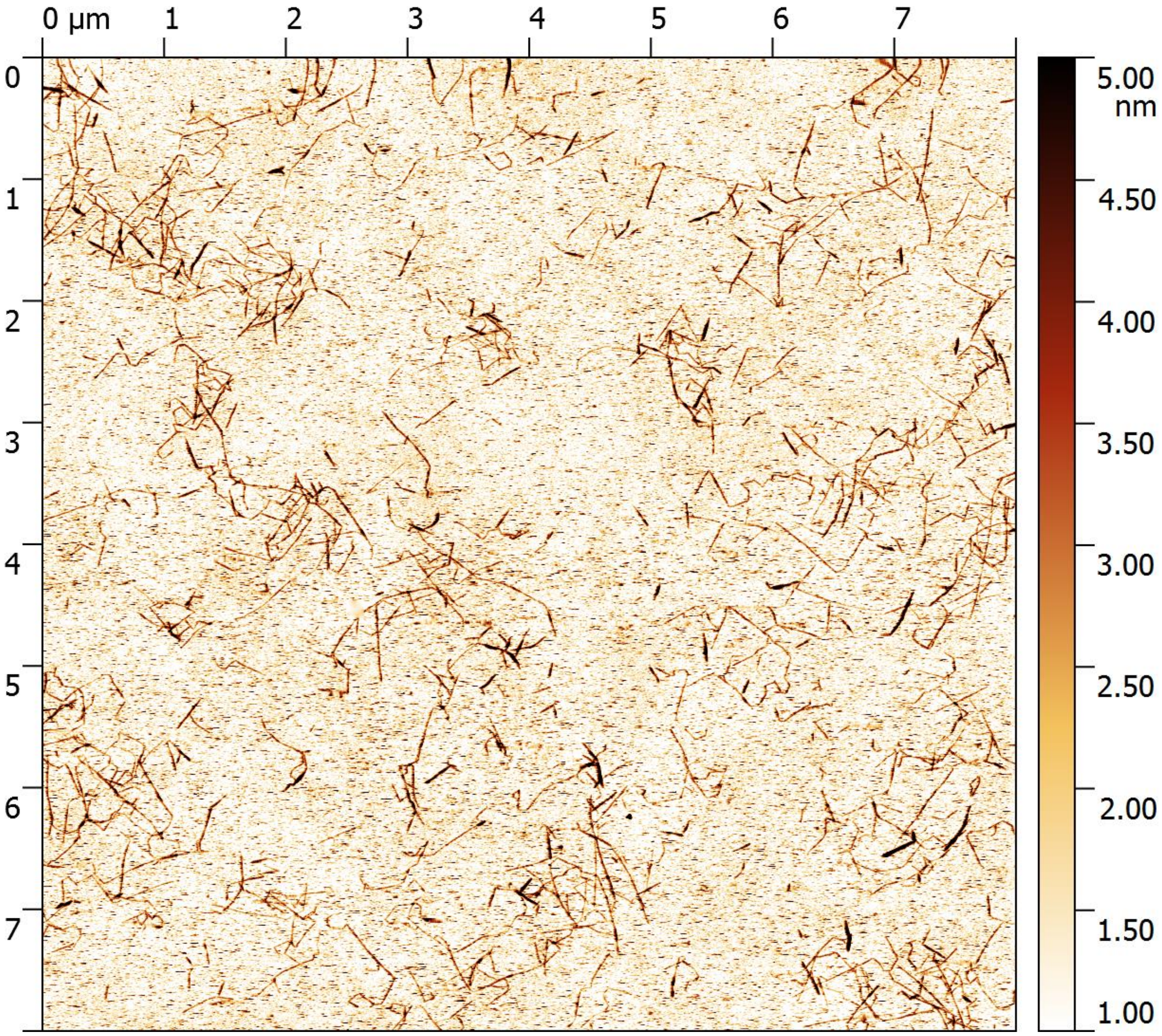

Figure S1. Representative AFM micrograph of TOCN used in this work. Color range has been adjusted to highlight the fibrils.

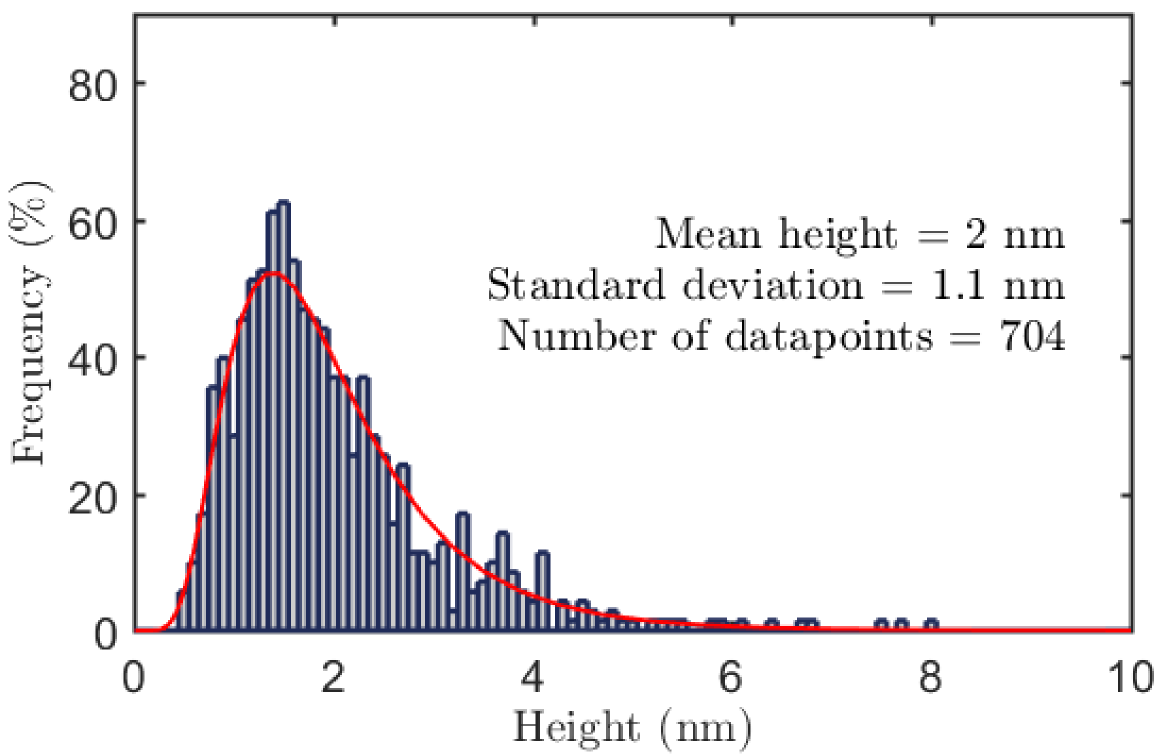

Figure S2. Lateral dimension distribution from AFM data (grey bars) of TOCN used in this work and a log-normal model distribution (red curve) fitted to the data.

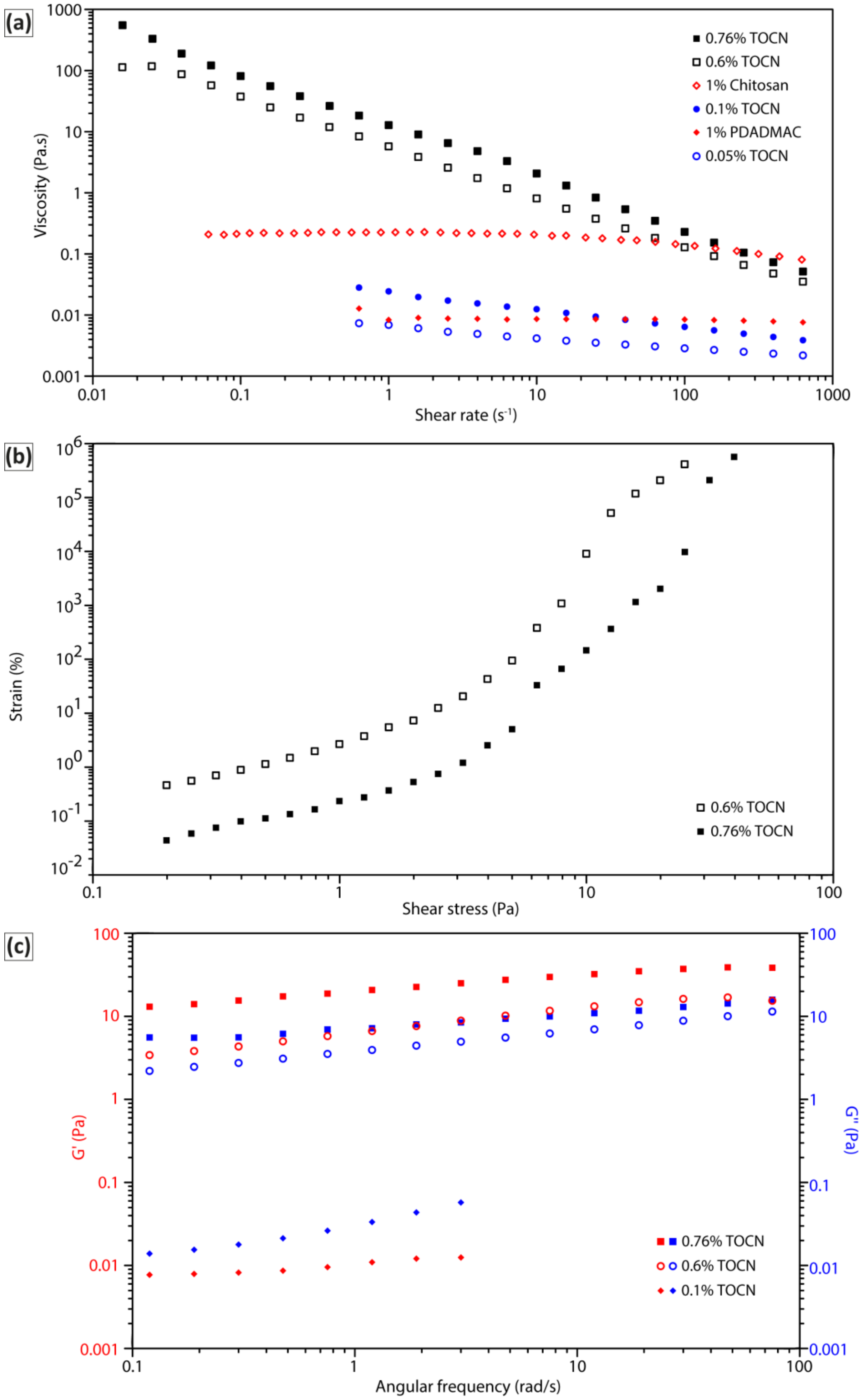

Figure S3. Rheological characterization of (a) viscosity vs. shear rate of TOCN dispersions and 1 wt. % polycation solutions used, (b) shear strain vs. shear stress of two TOCN dispersions, and (c) *G*' and *G*'' of TOCN dispersions vs. angular frequency.

TOCN/polycation (This work)	Type of CNF	Prestretch (%)	Young's modulus (GPa)	Yield strength (MPa)	Ultimate tensile strength (MPa)	Strain at break (%)	Diameter (µm)
PDADMAC-0%, N = 5	TEMPO-Ox.	0	15 (1)	98 (16)	204 (20)	7.6 (1.4)	53.7 (5.9)
PDADMAC-20%, N = 4	TEMPO-Ox.	20	23 (5)	133 (8)	240 (11)	4.1 (1.0)	47.8 (6.2)
Chitosan-0%, N = 5	TEMPO-Ox.	0	15 (1)	90 (4)	198 (4)	9.2 (0.9)	62.0 (3.7)
Chitosan-20%, N = 5	TEMPO-Ox.	20	20 (2)	125 (5)	250 (10)	5.4 (0.4)	58.6 (2.0)
Iwamoto *et al.*[15]	TEMPO-Ox.	0	24 (2)	-	321 (145)	2.2 (1.2)	
Walther *et al.*[16]	TEMPO-Ox.	0	23 (0.4)	175**	275 (15)	4.0 (0.2)	
Torres-Rendon *et al.* [17]	TEMPO-Ox.	0	8.2 (2)	75**	118 (12)	8.3 (2.9)	
Torres-Rendon *et al.* [17]	TEMPO-Ox.	28	34 (4))	225**	289 (34)	1.6 (0.3)	
Håkansson *et al.*[18]	Carboxy-methylated	0*	18 (1)	270**	490 (86)	6.4 (1.6)	
Hooshmand *et al.*[20]	Unmodified	0	11 (1)	150**	198 (11)	3.6 (0.6)	

Table S1. Mechanical properties of fibers prepared in this work and in the related literature. Values in brackets are the standard deviations of the corresponding values. In the first column N is the number of specimens that were analyzed for that sample. *Orientation of fibrils during flow prior to coagulation. **Yield strength not given numerically and estimated from stress-strain curve.

	PDADMAC (wt. %)						Chitosan (wt. %)		
TOCN (wt. %)	20	6	2	1	0.2	0.02	1	0.2	0.02
0.025	No	No	No	No	Yes	Yes	Yes	Yes	Yes
0.05	No	No	No	Yes	Yes	Yes	Yes	Yes	Yes
0.1	Yes	Yes	Yes	Yes*	Yes	Yes	Yes	Yes	Yes
0.2	Yes	Yes	Yes*	Yes*	Yes*	Yes	Yes	Yes	Yes
0.4	Yes	Yes	Yes*	Yes*	Yes*	Yes	Yes*	Yes*	Yes
0.6	No	No	Yes	Yes*	Yes*	Yes	Yes*	Yes*	Yes
0.7	No	No	No	No	Yes	Yes	Yes	Yes	Yes
0.76	No	No	No	No	No	No	Yes	Yes	Yes

Table S2. Feasibility of fiber spinning from the interface between adjacent droplets of TOCN and polycation at various combinations of concentrations. * = The combination of concentration marked with an asterisk were subjectively evaluated to be the most robust for IPC spinning purposes.

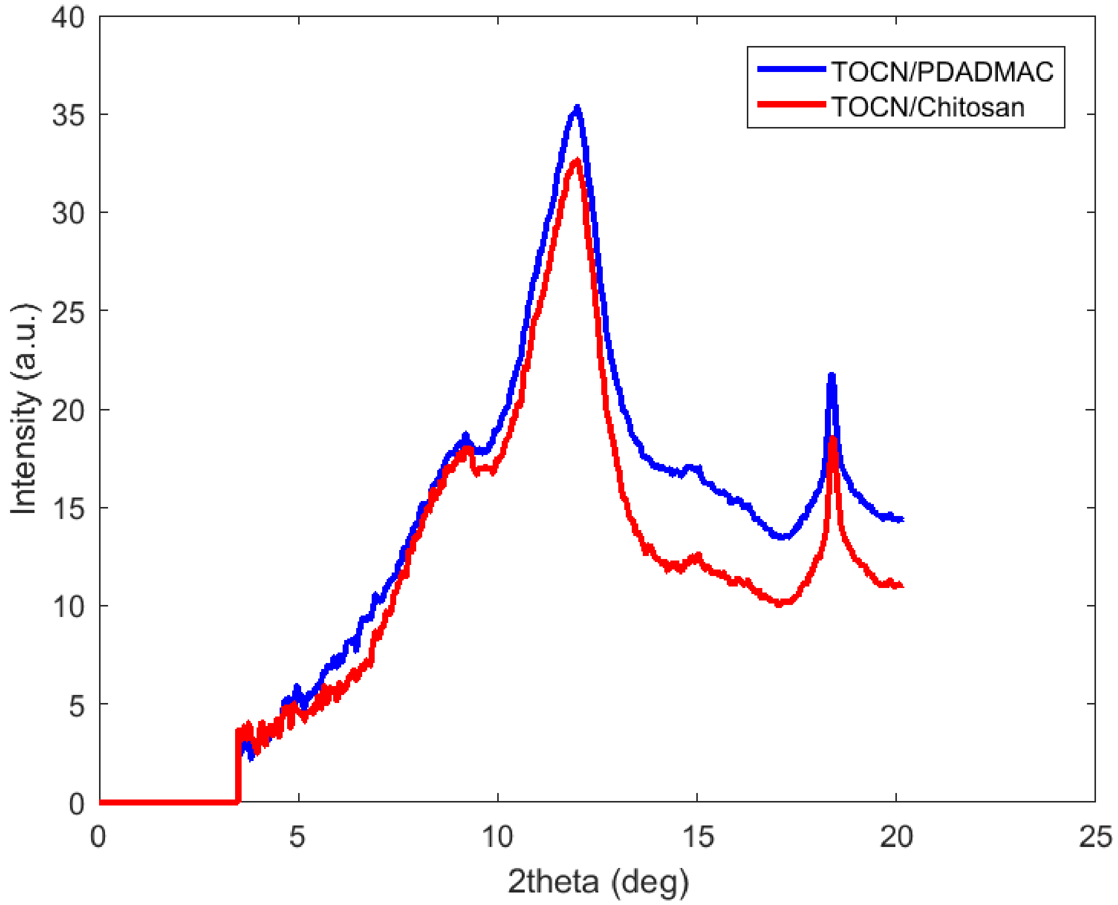

Figure S4. Radial intensity profiles of WAXS diffractograms of a TOCN/PDADMAC and a TOCN/Chitosan fiber. The intensity profiles display clearly the similar shape which comes from the TOCN component. This further supports the claim that the fiber is mostly composed of TOCN and the polycation is only a minor component because the scattering contribution is directly proportional to the fraction of each component present.

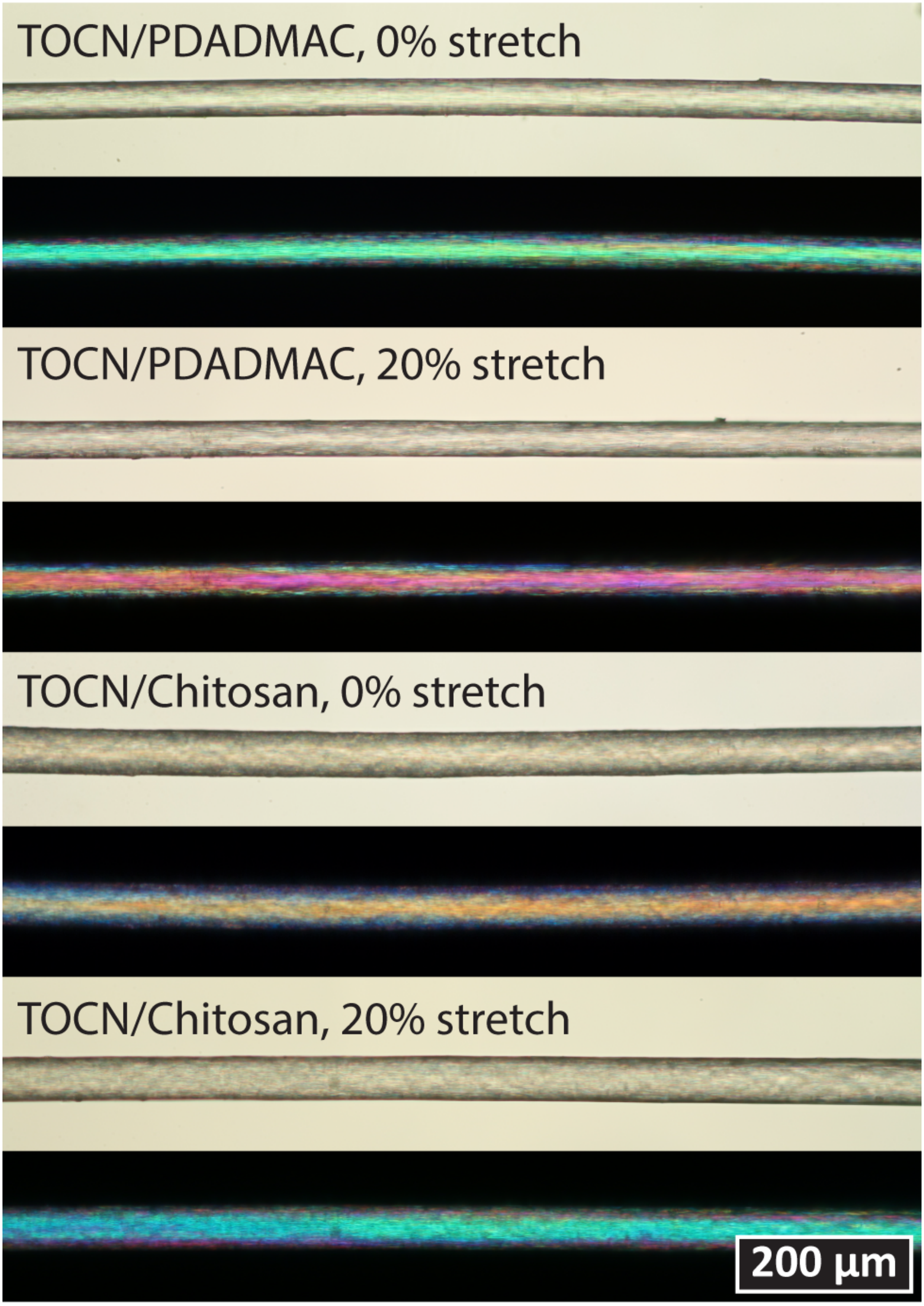

Figure S5. Optical microscopy of TOCN/polycation fibers with and without crossed polarizers at 45° angle to the fiber axis.

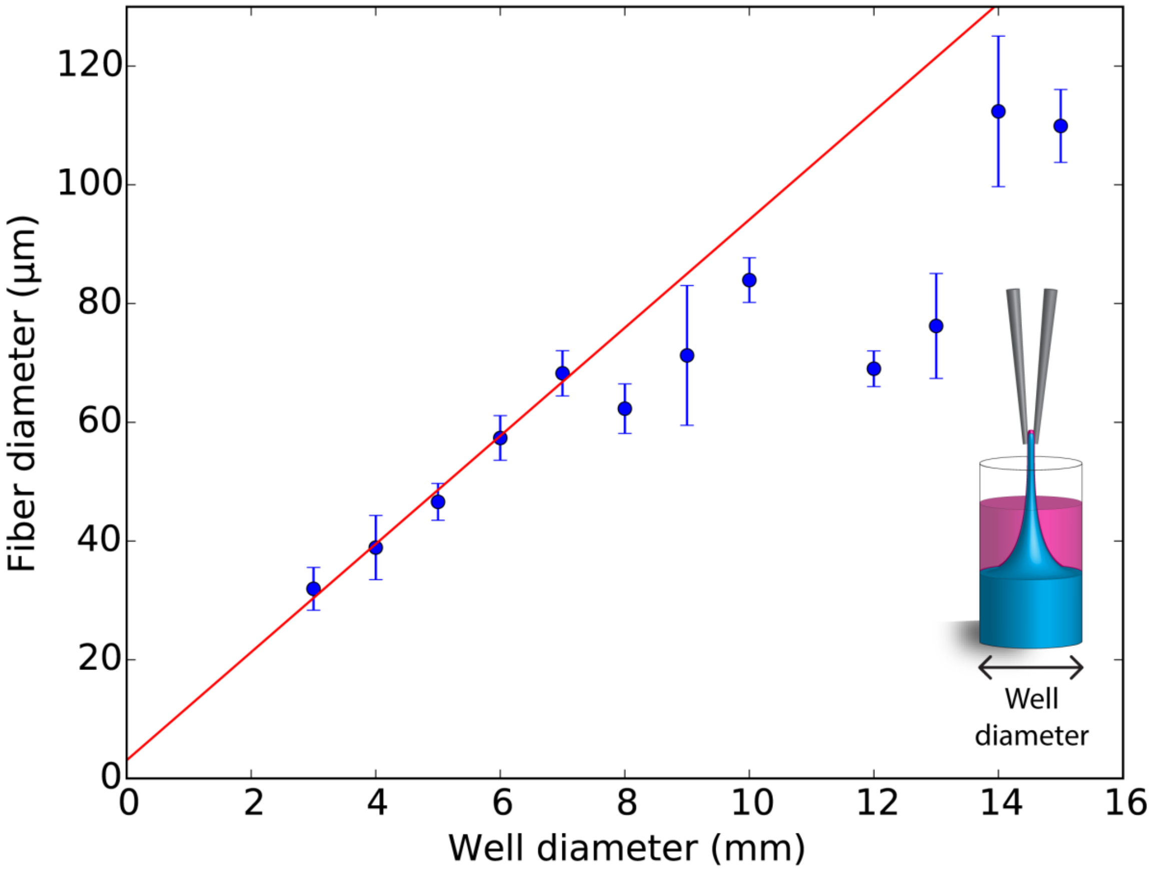

Figure S6. Effect of diameter of well used to spin the fiber on the diameter of the resulting dried TOCN/Chitosan fiber. Inset shows schematically setup used for IPC spinning.

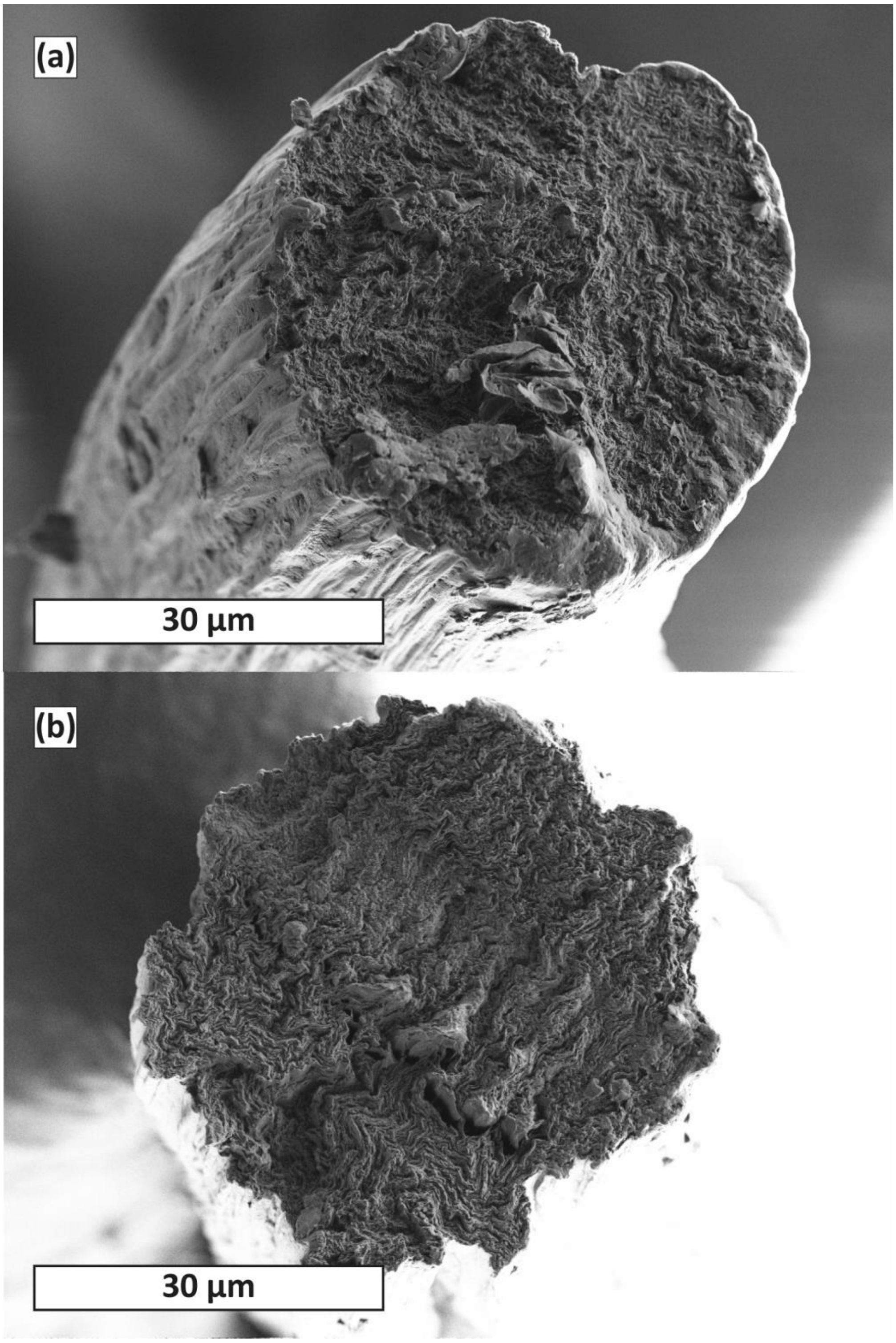

Figure S7. SEM micrographs of cross-sectional fracture surfaces of (a) TOCN/Chitosan, and (b) TOCN/ PDADMAC fibers. The images are the same as in the insets in Figure 5(a) and (d) in the main text. The reader is urged to magnify to the images in the electronic version in order to see the thin coacervate skin. Especially in (a) the skin can be seen on some edges of the cross-section to have collapsed as a thin membrane on the TOCN-core.

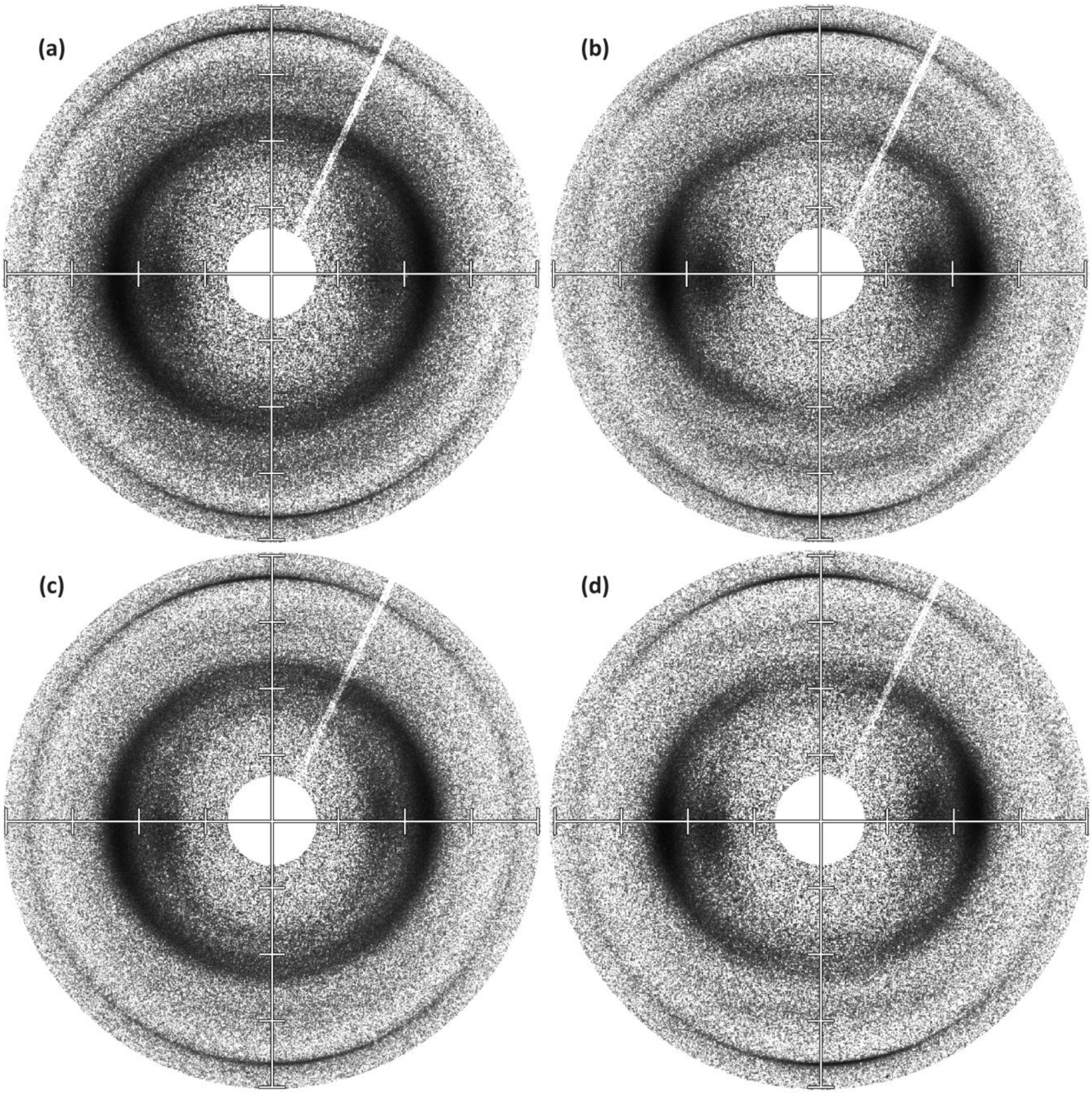

Figure S8. WAXS-diffractograms of TOCN/Chitosan fibers stretched to (a) 0 % and (b) 20 % strain and TOCN/PDADMAC fibers with (c) 0 % and (d) 20 % strain of the wet filament prior to drying. The ticks in the axes are located at values of 5, 10, 15 and 20 degrees for 2θ.

	Prestretch (%)	HOP* (S)	FWMH**	Degree of orientation (Π)
TOCN/PDADMAC	0	0.425 (0.048)	37.83 (5.49)	0.790 (0.031)
TOCN/PDADMAC	20	0.488 (0.085)	28.92 (1.24)	0.839 (0.007)
TOCN/Chitosan	0	0.434 (0.060)	46.17 (8.23)	0.744 (0.046)
TOCN/Chitosan	20	0.488 (0.057)	26.42 (1.56)	0.853 (0.009)

Table S3. Orientation parameters calculated from diffractograms of TOCN/polycation fibers. Reported values are calculated from two individual fibers of each type and diffractograms taken from three separate locations on each fibers and utilizing the azimuth intensity profiles in two sets, thus averaging over 12 computed values of each type. Values in brackets are the standard deviations of the corresponding values. *HOP = Hermans orientation parameter. **FWMH = Full-Width Medium Height.

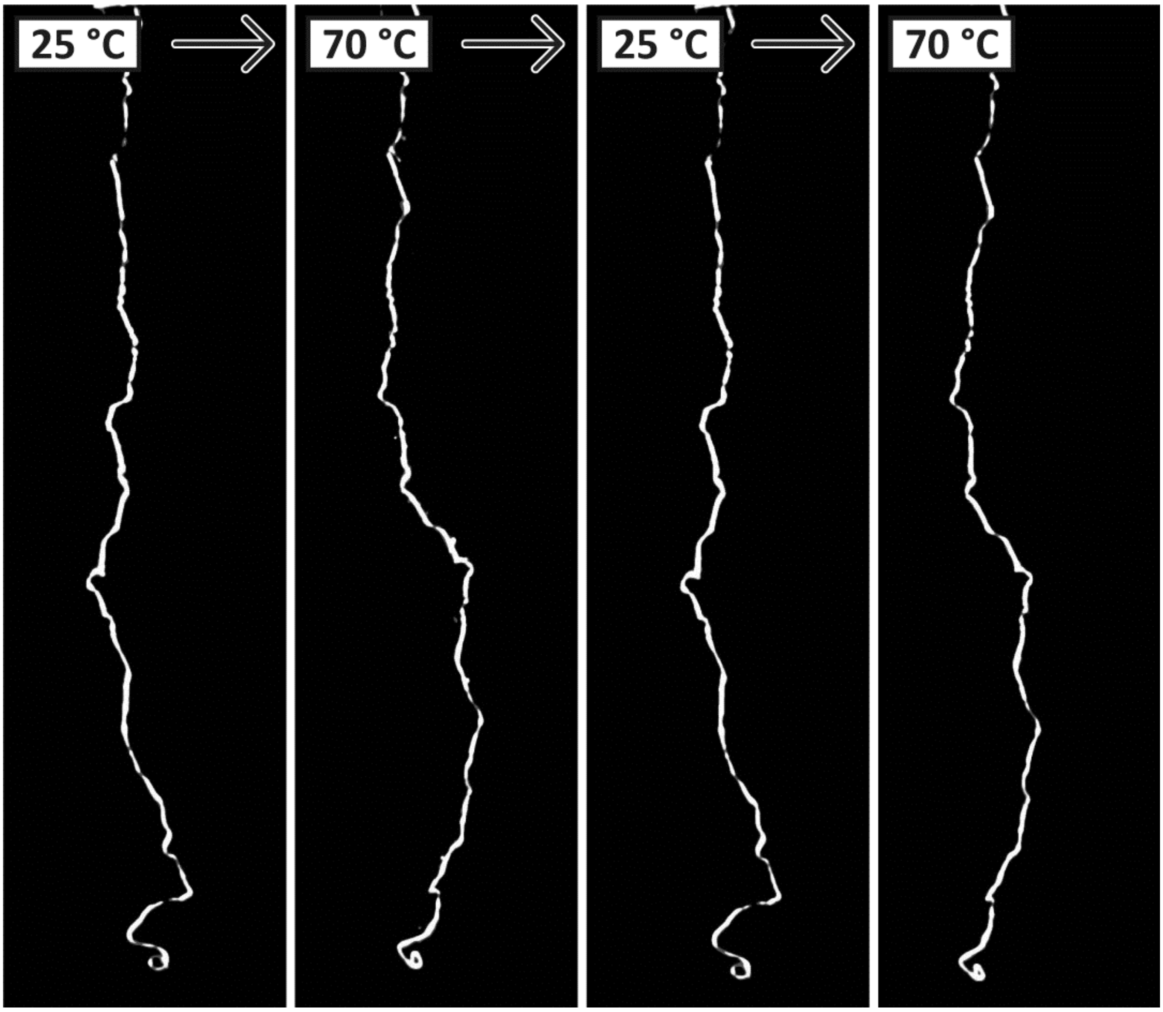

Figure S9. Photographs of bicomponent fiber (chitosan-oleate fiber wound with a TOCN/Chitosan) at low absolute humidity corresponding to 10 % relative humidity at 20 °C upon cycling of temperature. The fiber was suspended vertically with one end attached to the hotplate used to apply heat. The contrast has been increased artificially for clarity. The length of the fiber shown is approximately 20 cm and has a diameter 50 µm.